

THERMOHYDRAULIC CHARACTERIZATION OF ADDITIVE MANUFACTURED HEAT EXCHANGERS USING LATTICE STRUCTURE

Aurélien CONROZIER¹, Damien SERRET¹, Jean-Michel HUGO¹

¹ TEMISTh SAS, Bâtiment TEAM Henri-Fabre, zone des Florides, 13700 Marignane, France

ABSTRACT

In this paper, we will present a study dealing the optimization of heat exchanger such as cold plate using additive manufacturing. The development of a porous approach to design heat exchanger is presented.

INTRODUCTION

Additive manufacturing is opening new possibilities to produce complex structures and is offering a huge potential of disrupting the industrial world. From a numerical file, it's possible to produce a real part in several materials in a couple of hours or days with only one machine. It seems possible to modify as it wishes the geometry without modifying the entire production line. According to market study (Magistrelli, 2019), aeronautics, space and defense domains still inseparables with additive. The additive market sold for 10 billion dollars of products and services in 2018. 17.7% for the precited domains. However, some issues must be solved as well as certification and process qualification and at this time the price of a part.

Heat exchangers and thermal applications are widely used in the industry and are appearing as a high potential application for additive manufacturing. Depending on the domains of use, Heat exchanger can be named cold-plate for electronic cooling, radiator, heat sink, heat pipe etc.

In space industry, thermal applications are challenged on several points: Performances in steady and transient modes, weight, compactness, reliability and systems integration. For the performances, AM appears very interesting. Using simulation tools, it's possible to create shape that will provides better performances (Figure 1) of including other functions such as heat storage. AM can also be used for a better integration of the heat exchanger, for example by curving the global shape to fit to a casing space.

Integrating additive manufacturing in the development of component need a new way to design systems and to have an overview of it. First, in the economic point of view, AM must be taken in the entire value chain, from the conception to stock management and parts evolutions. In term of part design, AM must consider transverse domains. In the case of thermal application, engineers must have an overview of all the systems. For this, engineers need efficient numerical tools and methodology to be able to provide optimized solutions (HUGO, HEWAM – Heat Exchanger With Additive Manufacturing, 2019) - Figure 3

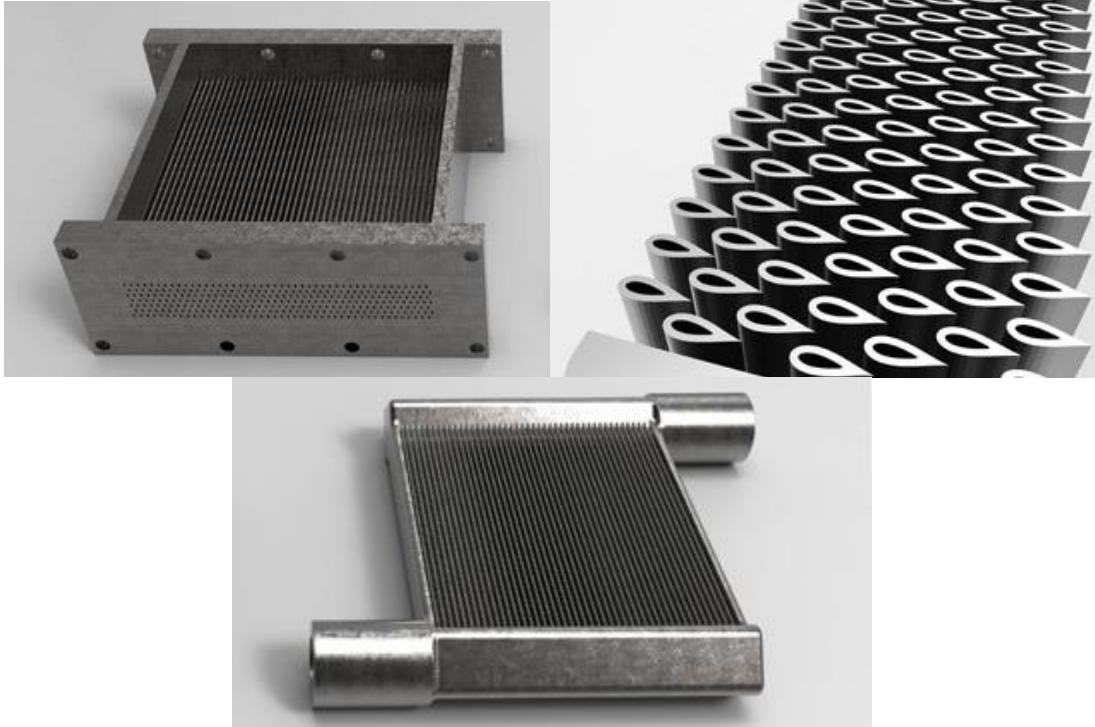


Figure 1 : Optimization of micro channel heat exchanger from University of Maryland (LANGNAU, 2016).

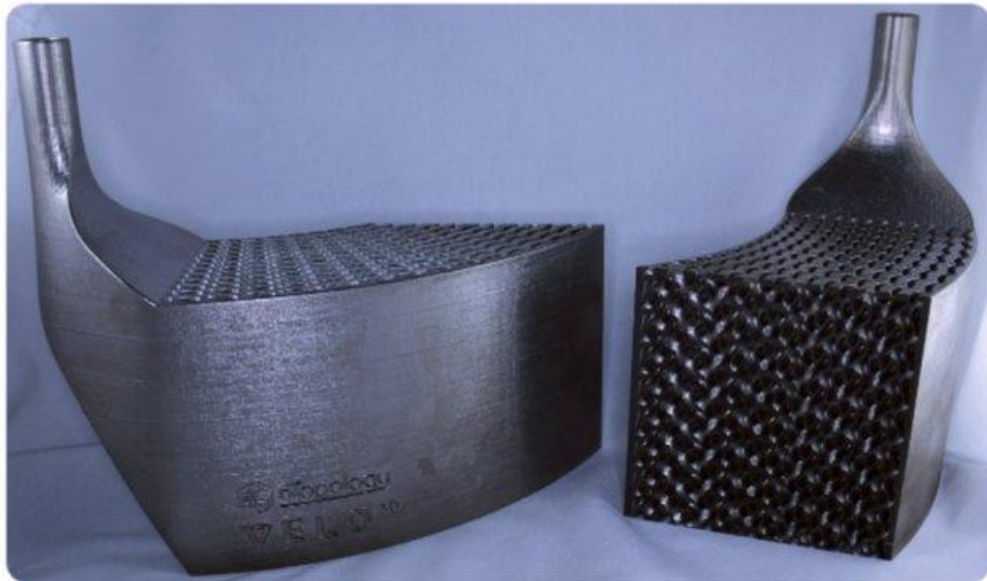


Figure 2. Additive heat exchanger using additive manufacturing with a curved shape and lattice structures (Velo3D, 2018)

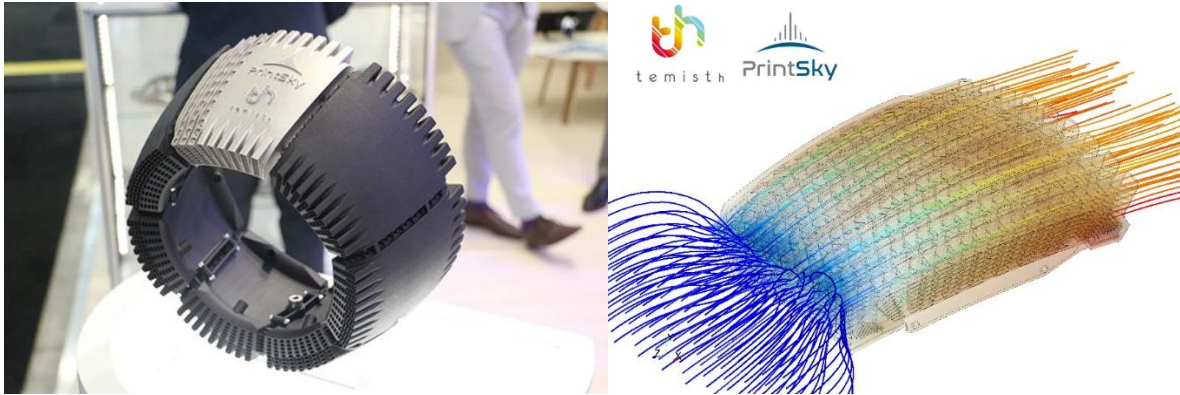


Figure 3. Modular Heat exchanger made by additive manufacturing on Form'Up 350 from AddUp and developed by Sogclair and Temisth

In this paper, we are presenting a study case of cold plate optimization using a numerical methods and materials dedicated to additive manufacturing process. Cold plates are usually used for electronic cooling. In this study we will use arbitrary chosen requirements and show how the propose methodology helps to improve a geometry in terms of thermal efficiency, fluid circulation and weight.

SCALE CHANGE METHODOLOGY AND CFD MODEL

Scale change approach for heat exchanger

Modeling heat exchanger using classical CFD allows obtaining many information such as local field of temperature, velocity or pressure and have a good understanding of heat transfer. It's a powerful tool for the design. The geometry change can be made easily. However, CFD have some limitation that we can neglect in the design of Heat exchanger, moreover for additive manufacturing.

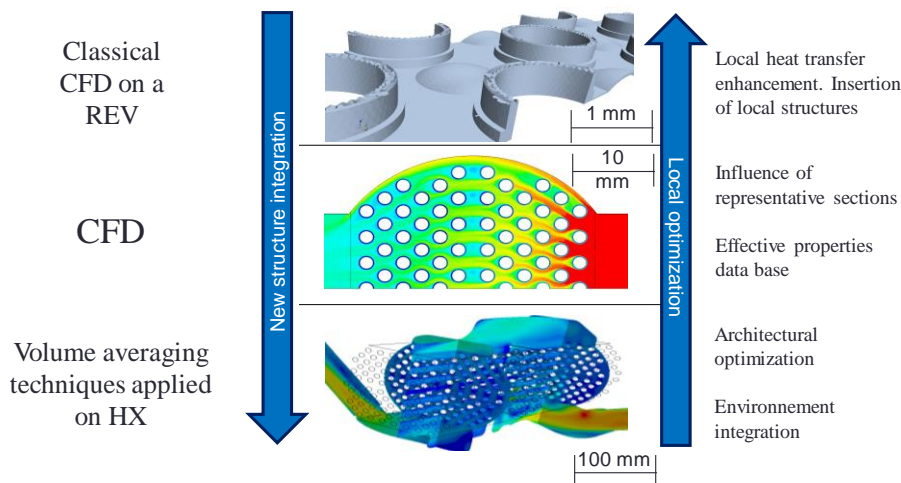


Figure 4. Different scales approaches for modeling heat exchanger.

First, in terms of physical model. CFD models are easily applied for monophasic fluid flow, laminar or turbulent with or without RANS model for the turbulence. However, these models don't take into account surface roughness easily. The simulations are usually made on a slip surface and geometrically perfect. Additive manufacturing parts have generally, a particular surface roughness due to the printer parameters, powder and surface orientation. Modeling the roughness in the case of heat transfer and fluid flow needs a direct simulation or simplify model. For example, using RANS Model two parameters can be used: roughness height that generates a shear stress on the surface and the turbulent Prandtl number for the heat transfer enhancement. However, in this method experiment are needed. The correlation between these parameters and surface roughness will be deduced after experiments. In the case of direct simulation, an accurate geometry that represent the roughness must be obtain (with μ CT or generated on CAD Software). This last method needs a small volume of interest in order to have a thin mesh that will capture the variation on the surface. In any case it took an important CPU time.

Using a model of roughness will not be enough to model easily a whole heat exchanger. Heat exchanger are made of several parts with different size. Collectors and distributors can be tubes of 100mm diameter. Channel are 2 o 3mm height, fins 0.3thickness etc. Mesh size for CFD must adapt to all this length. A strategy that can be used is to perform a simulation on a elementary channel and a global simulation replacing the heat transfer area by a porous media.

An equivalent porous approach: Two temperatures models

We propose to design the heat exchanger using a two-temperatures model coupled with a porous media approach (Whitaker, 1998; HUGO, Transferts dans les milieux cellulaires à forte porosité : applications à l'optimisation structurale des échangeurs à ailettes, 2012). In this model, fins or lattice structure will be replaced by an equivalent and homogeneous media with several sources that generate heat transfer and pressure drop. For a cold plate, the structure of heat transfer intensification, such as Lattice of metal foam, we be replace by two porous media, one for the fluid using a Forchheimer-Darcy law and one the heat conduction in the solid. The model of heat transfer is described by the following equations:

$$\begin{aligned} \varepsilon(\rho C_p)_f \frac{\partial T_f}{\partial t} + \varepsilon(\rho C_p)_f \mathbf{U} \cdot \nabla T_f &= \nabla \cdot (\lambda_f^{eff} \nabla T_f) + h S_p (T_f - T_s) \\ (1 - \varepsilon)(\rho C_p)_s \frac{\partial T_s}{\partial t} &= \nabla \cdot (\lambda_s^{eff} \nabla T_s) + h S_p (T_s - T_f) \end{aligned} \quad (1)$$

Where $\varepsilon(-)$ is the porosity of the structures, ρC_p (J/m³K) is the heat capacity times density, T(K) the temperature, U(m/s) the velocity of fluid, λ^{eff} (W/mK) the effective thermal conductivity, Sp(m⁻¹) the specific surface and h(W/m²K) the heat transfer coefficient. Index f and s are respectively used for fluid and solid.

The model of pressure drop is described by the Darcy-Forchheimer law :

$$-\nabla P = \frac{\mu}{K} \mathbf{U} + \rho \beta \|\mathbf{U}\| \mathbf{U} \quad (2)$$

Where ∇P (Pa/m) is the lineic pressure drop, \mathbf{U} (m/s) the fluid velocity, μ (Pa.s) the fluid viscosity, ρ (kg/m³) the fluid density, K (m²) and β (m⁻¹) are respectively the permeability and the inertial coefficient of the porous medium.

K and β are both independent from the fluid crossing the porous medium and just depend on the structure. They are represented by a matrix:

$$\overline{\overline{K^{-1}}} = \begin{bmatrix} K_{xx} & K_{xy} & K_{xz} \\ K_{yx} & K_{yy} & K_{yz} \\ K_{zx} & K_{zy} & K_{zz} \end{bmatrix} \quad (3)$$

These matrices are usually symmetric. Non diagonal component can have a positive value if the geometry is not symmetric (i.e. a wing that generates a vertical force for a horizontal velocity). One difficulty using this model is that the value of the component depends on the fluid flow direction. The following pictures illustrate the phenomenon for an array of pin fins usually used for heat transfer intensification in cold plates.

Figure 5 shows an example of pin fins array with a constant pattern in two directions. This pattern is clearly presenting two preferential directions for the fluid flow where the number of obstacles reach by fluid particle is minimum. To illustrate this, we carry out a simulation using a CFD commercial software (StarCCM+). In order to obtain all the direction, we cut the array randomly with an arc of circle respecting some rules: The inside diameter must be enough big for catching an amount of at least five patterns. In the same way, the fluid must cross at least 3 or 5 patterns in order to be representative. Velocity fluid is imposed at the inside diameter. Pressure outlet is imposed at the outside diameter. Pins are walls and other surface are symmetry.

Figure 6 shows velocity profiles on outlet surface. We clearly observe that there is two maximal velocity for 0 and 90 degrees that correspond to the maximal aperture of the flow. Two minimal velocity are observed for 30 and 60 degrees. Another maximal velocity is observed for 45 degrees. The value of permeability and inertial coefficient have to take into account the fluid flow direction.

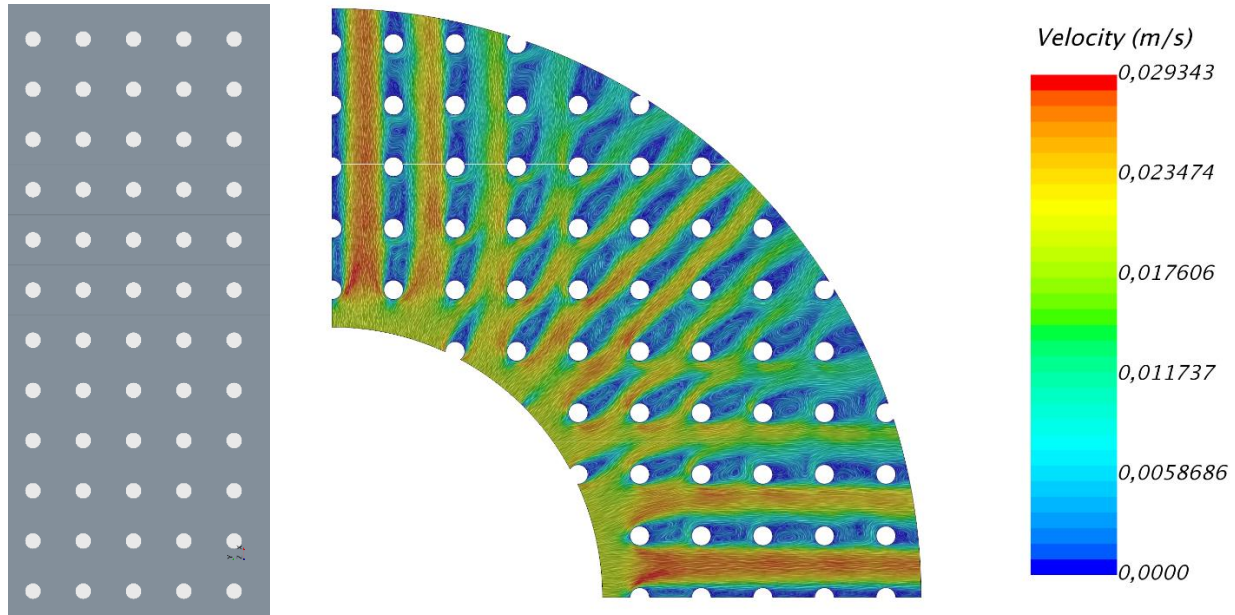


Figure 5. On the left : classical array of pin fins used for heat transfer intensification in cold plates. On the right: velocity field on a circular sample randomly cut in this array.

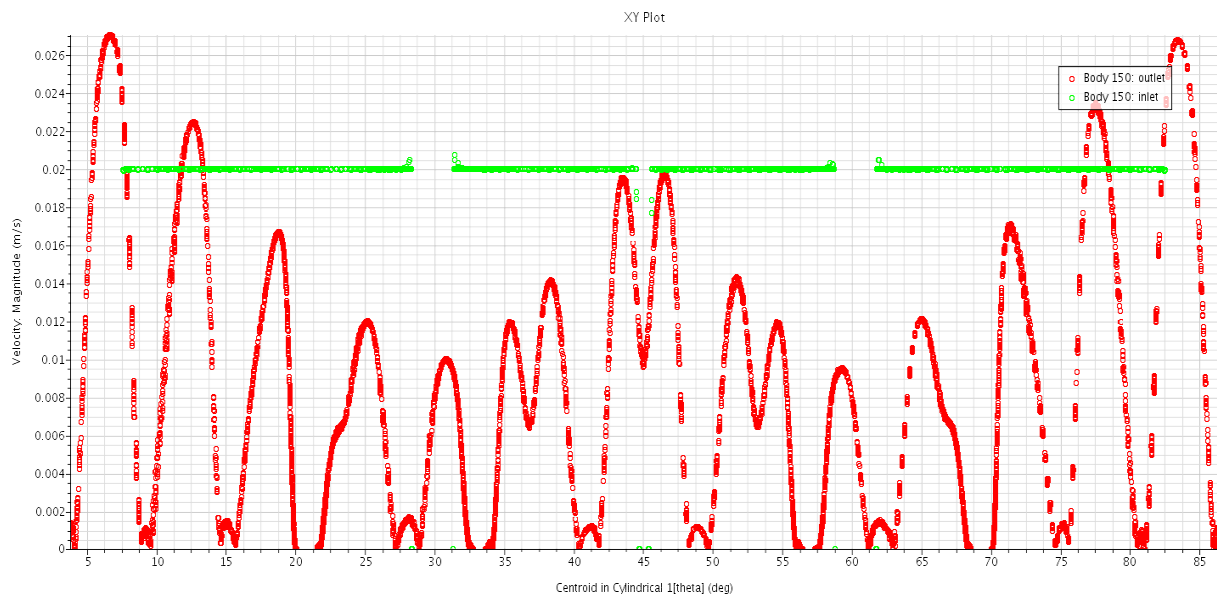


Figure 6. Velocity profiles on inlet (green dot line) and outlet (red dot line) surface versus the orientation angle of the surface.

Using a spherical coordinates system can be used for considering the orientation of the fluid flow. Angle θ and γ described the orientation of fluid and its pressure drop. Orientation of pressure drop and fluid flow can be different in the case of non-symmetric structure (i.e. winglet).

$$-\begin{pmatrix} \|\nabla P\| \\ \theta_p \\ \gamma_p \end{pmatrix} = \mu \overline{K}^{-1} \begin{pmatrix} \|\mathbf{U}\| \\ \theta_u \\ \gamma_u \end{pmatrix} + \rho \overline{\beta} \|\mathbf{U}\| \begin{pmatrix} \|\mathbf{U}\| \\ \theta_u \\ \gamma_u \end{pmatrix} \quad (4)$$

For heat transfer intensification we have chosen a structure that can be used for its mechanical properties. We thus select a lattice structure called X. It's made of tubes following main diagonals of a cube and crossing themselves at the middle of the cube. The structures described in

Figure 7 is using two geometrical parameters "a" and "d". "a" is the size of the pattern. "d" the diameter of the strut.

In the following section, lattice characterization is described. We assume that structures used are homogeneous and isotropic.

Geometrical characterization of thermo-physical properties of lattice structure.

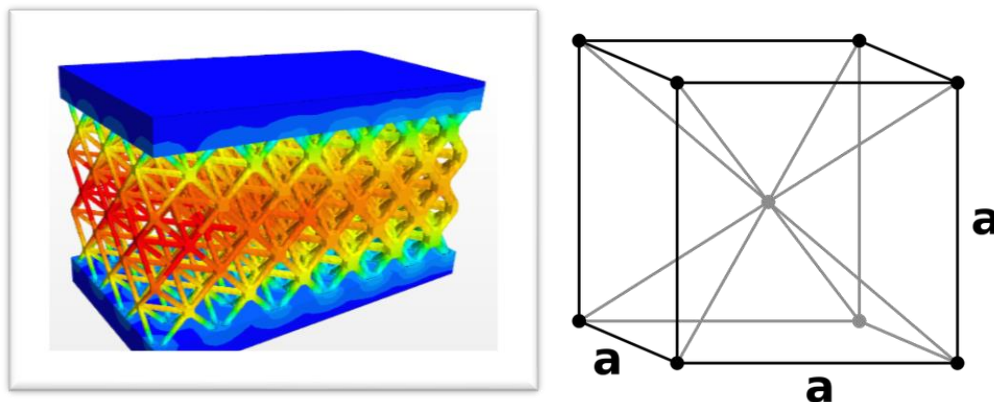


Figure 7. Description of a lattice X.

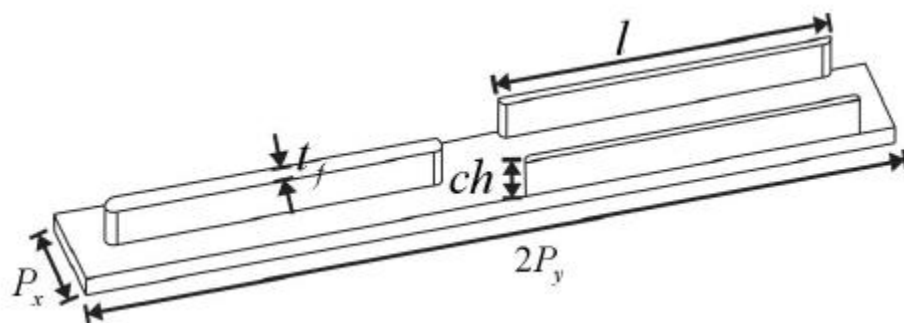


Figure 8. Example of structures usually used for cold plate: fin array

Optimization methodology – Lattice characterization

A classical sizing of heat exchanger and cold plate will first find the best couple of geometrical parameters. For example, for fins or pins array, pitches and diameter can be change in order to find the best compromise between heat transfer, pressure drop and mass.

Design a cold plate with a uniform pattern remains to use correlation like equation (5) and (6) that give non dimension heat transfer and pressure drop coefficients (CHEN, 2015)..

$$f = 9.6243R_e^{-0.7422}\beta^{-0.1856}\delta^{0.3053}\gamma^{-0.2659}(1 + 7.669 \cdot 10^{-8}R_e^{4.429}\beta^{0.92}\delta^{3.767}\gamma^{0.236})^{0.1} \quad (5)$$

$$j = 0.6522R_e^{-0.540}\beta^{-0.1541}\delta^{0.1499}\gamma^{-0.0678}(1 + 5.269 \cdot 10^{-5}R_e^{1.84}\beta^{0.504}\delta^{0.456}\gamma^{-1.055})^{0.1} \quad (6)$$

Where $j(-)$ is the Colburn number related to the heat transfer coefficient:

$$h = j \cdot \left(R_e \frac{P_r^{\frac{1}{3}}}{D_h} \right) \frac{\lambda_f}{D_h} \quad (7)$$

Où λ_f (W/mK) is the fluid thermal conductivity.

And :

$$\beta = \frac{P_x - t}{ch} \quad (8)$$

$$\delta = \frac{t_f}{l} \quad (9)$$

$$\gamma = \frac{t_f}{P_x - t_f} \quad (10)$$

Where ch (m) is the channel height, t_f (m) its width, l (m) is the fin length, P_x (m) the pitch length between two fin in the flow direction (

Figure 8).

In the same way, correlation can be found for lattice structure using two parameters. The following correlation are given for an equivalent porous approach as described below. For several ratio between a and d , we plot Nusselt number, Permeability, inertial coefficient and other parameter.

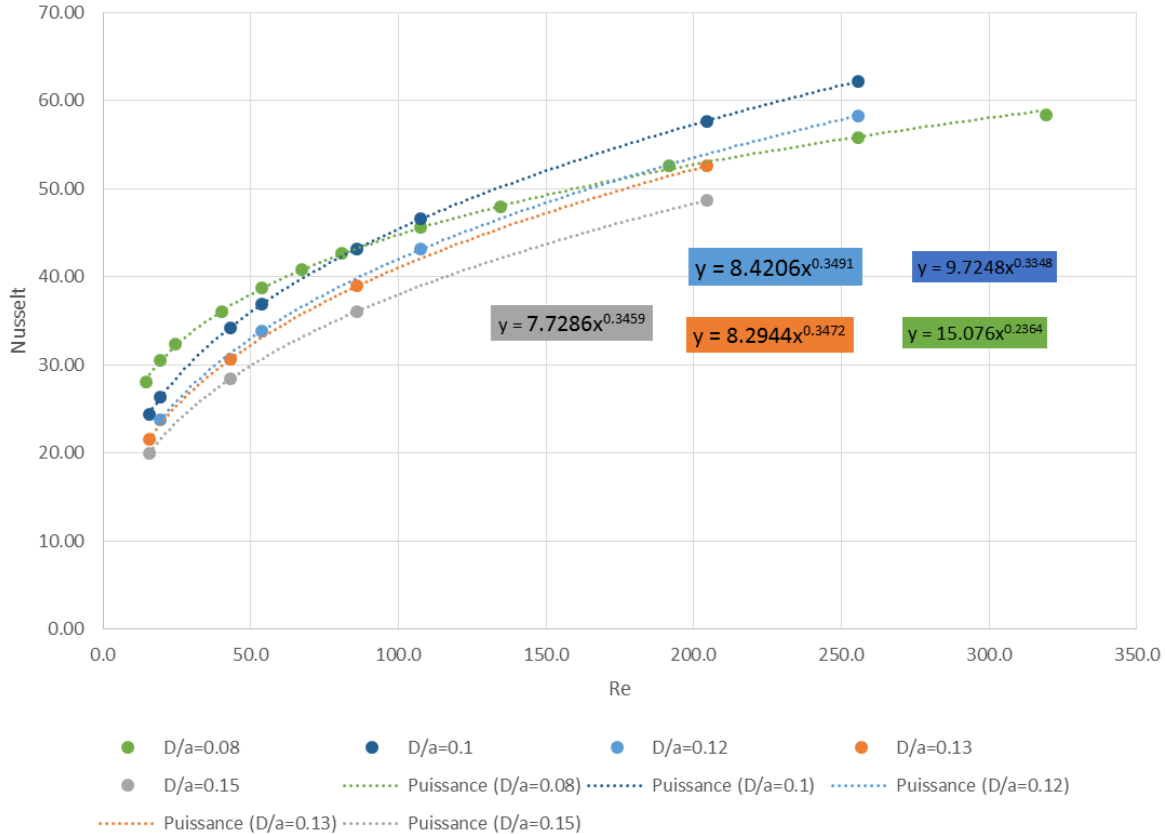


Figure 9. Nusselt number of local heat transfer coefficient (between fluid and strut) versus Reynolds number for several ratio of d/a .

For the Nusselt number calculated with parameter “a” of the lattice as the characteristic length versus the Reynolds number, we found several curves following a power law (Figure 9). For extracting a unique correlation, we then plot the coefficient of proportionality “alpha” and the exponent “n” of each curve versus the ratio of strut diameter “d” over lattice pattern “a”. We found correcting factor (Figure 10) that can be used to propose a correlation (11).

The same methodology can be used for proposing correlation for other parameters. Equation (12) give the developed surface per volume unit versus d over squared a . Equation (13) give the relationship of the apparent thermal conductivity as a polynomial law. Equation (14) give the relation for apparent density of the lattice structure and equations (15, 16 and 17) give the relation of pressure drop coefficients.

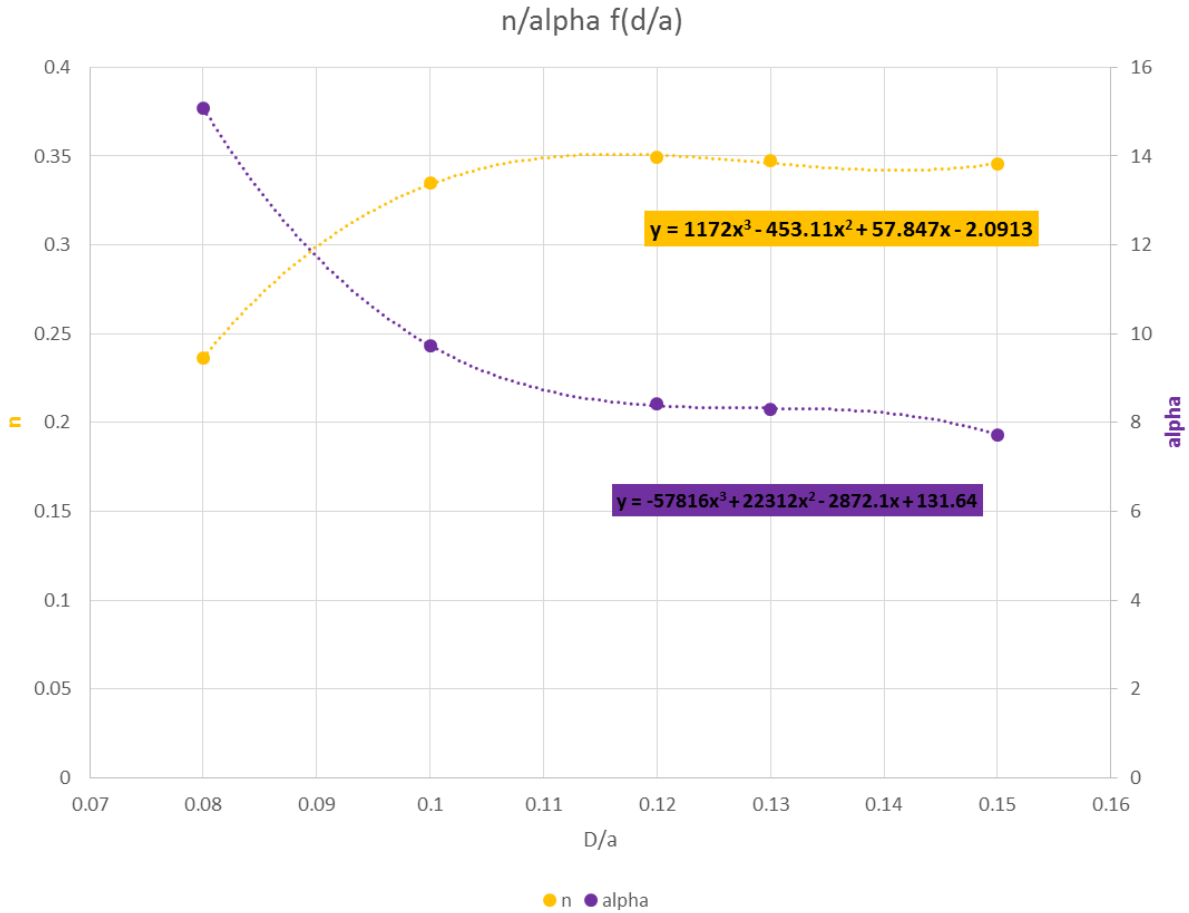


Figure 10. Correction factor for the Nusselt number depending on a and d.

$$Nu = \left(-15119,42 \left(\frac{D}{a} \right)^3 + 6021,27 \left(\frac{D}{a} \right)^2 - 802,88 \left(\frac{D}{a} \right) + 38,59 \right) Re^{\left(992,41 \left(\frac{D}{a} \right)^3 - 389,02 \left(\frac{D}{a} \right)^2 + 50,537 \left(\frac{D}{a} \right) - 1,8242 \right)} \cdot Pr^{1/3} \quad (11)$$

$$S_p = 17,756 \cdot \frac{D}{a^2} - 9,8198 \quad (12)$$

$$\lambda = 35,112 \cdot \left(\frac{D}{a} \right)^2 - 1,3288 \left(\frac{D}{a} \right) + 0,0498 \quad (13)$$

$$\rho_{eff} = 8681,5 \left(\frac{D}{a} \right) - 516,28 \quad (14)$$

$$f = \frac{A}{Re} + B \quad (15)$$

$$A = \frac{2a^2}{k} = -17140 \left(\frac{D}{a} \right)^2 + 8356 \left(\frac{D}{a} \right) - 310,56 \quad (16)$$

$$B = 2\beta a = 13,869 \left(\frac{D}{a} \right)^2 + 4,4082 \left(\frac{D}{a} \right) - 0,0115 \quad (17)$$

COLD PLATE OPTIMIZATION

In the following section, we show how an equivalent porous approach can be used for global optimization of a cold plate. We propose to solve an arbitrary requirement by proposing a global solution with an uniform pattern and then to modify locally the pattern in order to decrease junction temperature, pressure drop and device weight.

Arbitrary requirements

We choose to size a cold plate where are imposed several heat fluxes. The plate size is 120x70x10mm. As it can be used as a mechanical support, we can't change this size. The coolant fluid is oil ($C_p=2200\text{J/kg/K}$; Thermal conductivity = 0.13W/mK , density= 0.825 and viscosity= 0.083Pa.s). Mass flow rate is imposed and set up at 5 g/s

The fluid inlet and outlet configuration are shown on Figure 11. Coolant fluid inlet is positioned at the top and right of the plate with a horizontal pipe. The main flow in the cooling part is vertical. Outlet is horizontal on one side of the plate.

Three heat sources are imposed on the surface with different value. 50W on $30\times 30\text{mm}$ square surface area (represented by a circle on the figure), 10W on $20\times 20\text{mm}$ square area (represented by a square) and 5W on $70\times 20\text{mm}$ rectangle area (represented by a rectangle).

The objective is to ensure that the surface of the plate doesn't reach temperatures over 55°C . In the same time, we want to ensure the minimal pressure drop and weight.

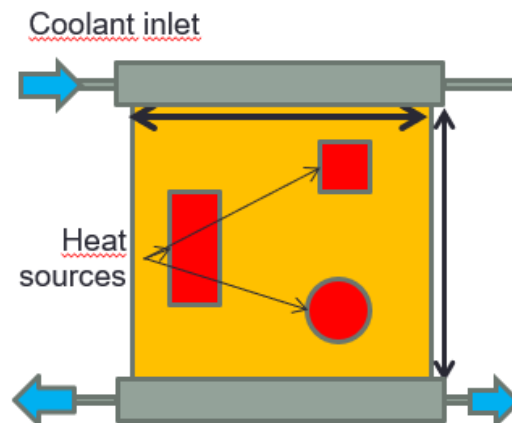


Figure 11. Cold plate example that is used for the optimization.

Cold plate sizing

From the correlation of lattice properties established in previous section we have chosen one couple of parameters "a" and "d" and then generate a homogeneous porous medium in the core

of the cold plate (Figure 12). The real geometry is then simulated on a commercial CFD software (StarCCM+ provides by Siemens).

Figure 13 shows a convolution of velocity vectors colored by their magnitude. We observe that the fluid has good repartition on the wall plate. Figure 14 shows the temperature field on the junction plane where heat fluxes are imposed. The main objective is obtained. Maximal temperature on one source remain under 50°C.

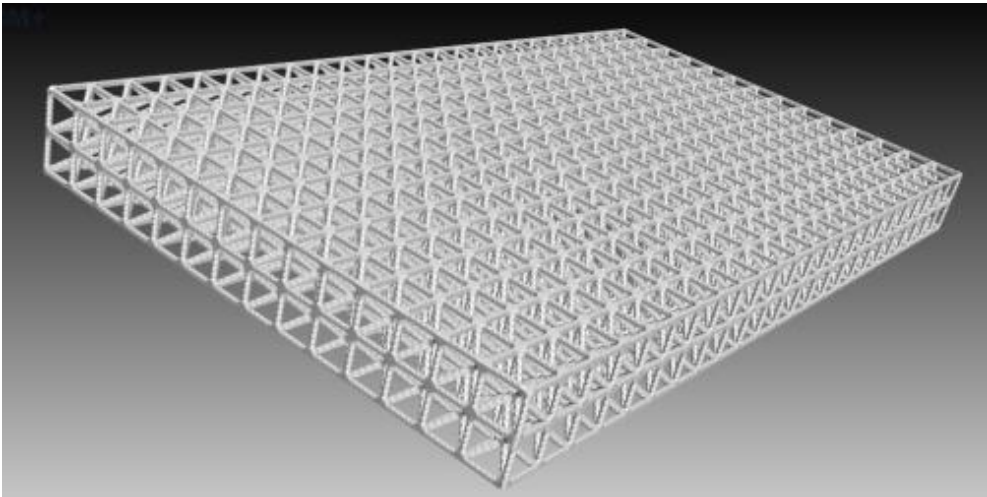


Figure 12. Homogeneous lattice structure inserted in the cold plate.

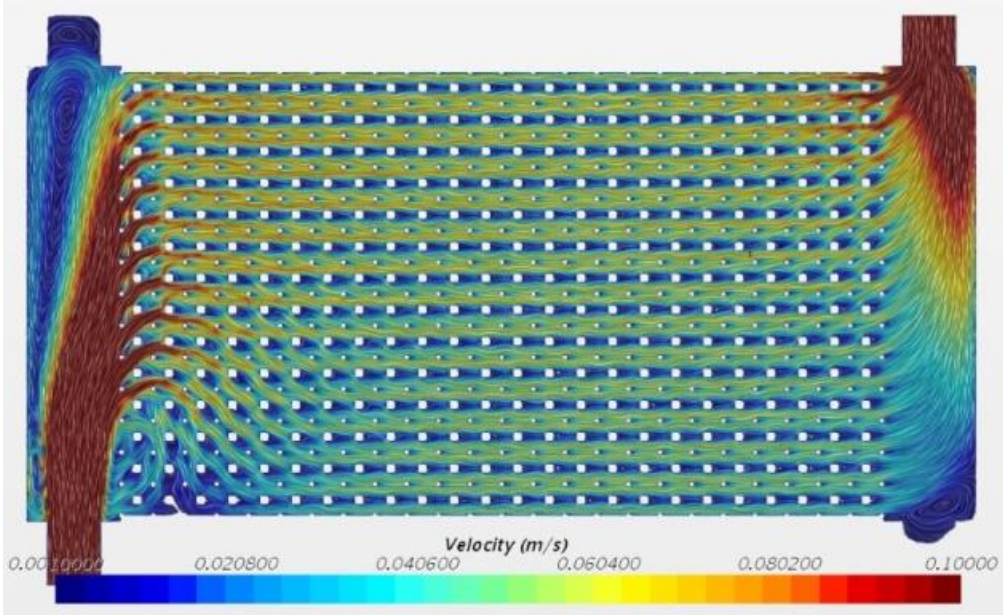


Figure 13. Velocity field in a plane section in the cold plate.

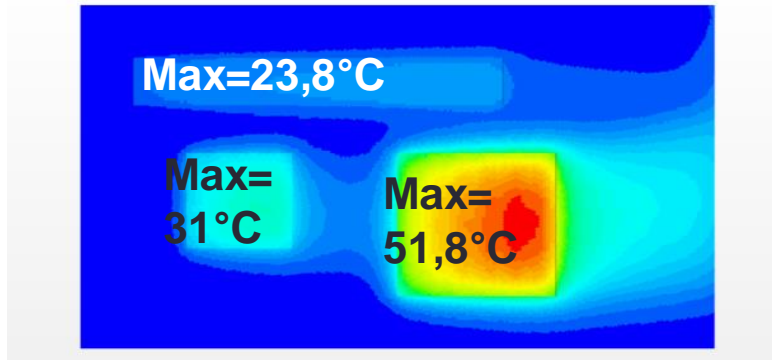


Figure 14. Surface of the heat source colored by the temperature.

This first sizing allows obtaining a satisfying solution to the requirements. However, this solution seems possible to improve. If we have a look to local results such a temperature field on Figure 14, we observe that only one source is closed to 55°C. First, this source is located at the end on the fluid flow where the fluid reaches its higher temperature. Then, this is the source with the higher heat flux. We can easily understand that an optimization can be done by changing local value of lattice parameter.

The value of the pattern is fixed, and the value of the strut diameter is fixed with a minimal value for mechanical reasons. The difficulties are to model the interaction between thermal improvement and fluid flow distribution. For example, increasing the struts size in the vicinity of the heat source will modify the fluid stream that will avoid the heat source. Using the porous approach with, the two temperatures model a variation of local performances can be done with a good prediction of the fluid flow. After several iterations we find a second solution shown in Figure 15 and Figure 16. In this solution we reduce the strut size of the lattice everywhere, except in the location on the maximal heat flux where a compromise is found between the thermal conductivity and the fluid permeability.

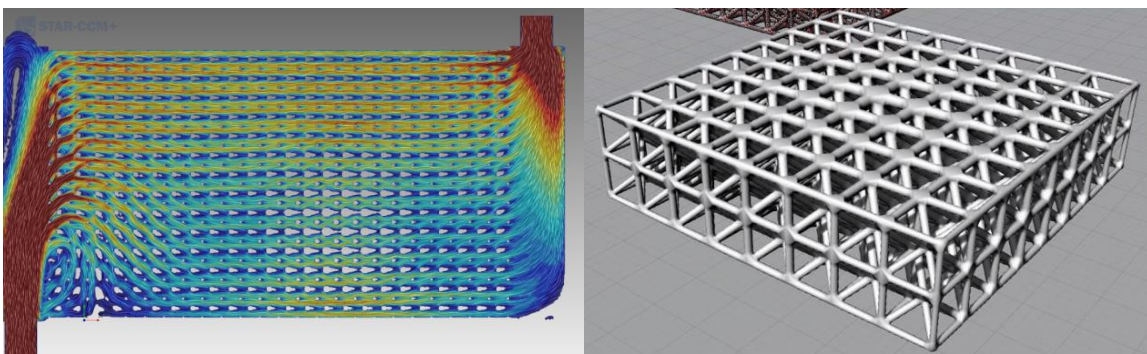


Figure 15. Second solution with local variation of the lattice structure.

Figure 16 shows that the temperature of two source has increased slightly however the maximal temperature has decreased from about 3°C. Moreover, local optimization of the structure allows

reducing the mass of the plate by 10% compared to global sizing and reduce the pressure drop by 7%.

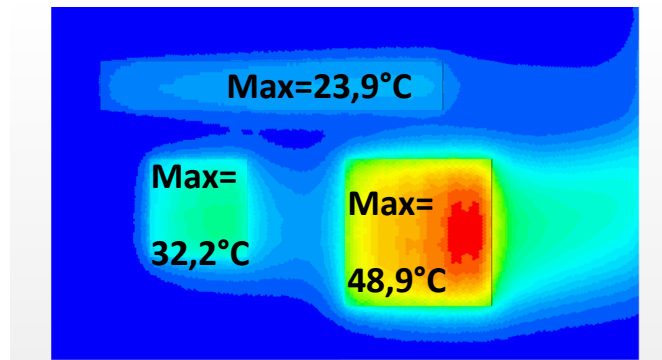


Figure 16. Second solution: temperature field improved.

Finally, the cold plate was built on a SLM280 in order to test feasibility. It is an open sample for the observation of the evolutive lattice (Figure 17).

Next work will consist on performing experimental tests with local measurement.

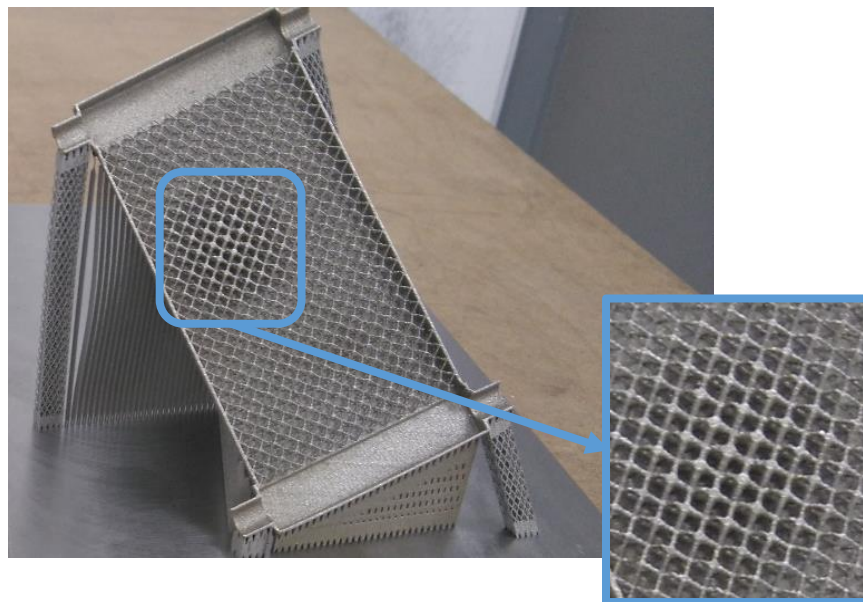


Figure 17. Cold-plate production on SLM280.

OTHER EXAMPLE OF APPLICATION

The methodology can be used in several situations. Figure 18 shows another example of application on a curved heat exchanger for electric engine cooling. The channel shape imposes a height variation for the fluid flow section. The porous approach helps in choosing the lattice structure:

- preferential path on the direction perpendicular to fluid inlet in order to have a good distribution of fluid.
- a progressive strut diameter in order to conserve the porosity.

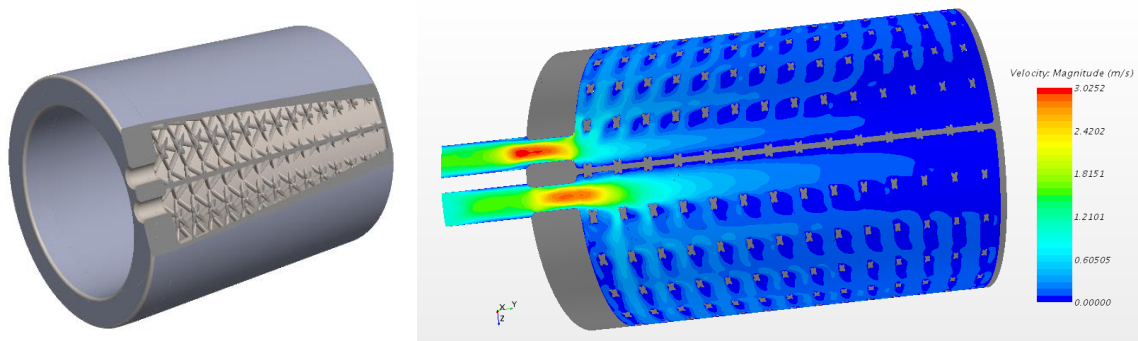


Figure 18. Example of application of AM heat exchanger: a curved cold-plate.

CONCLUSIONS

Additive manufacturing opens a wide range of opportunities for thermal systems. From a numerical 3D CAD and only one machine it's possible to create a very complex shape adapted to the available casing for the system and adapted to the physical phenomenon.

In this paper, we have shown that theory of porous media can be applied to heat exchanger as well as cold-plate. We perform an optimization on a simple square plate. We gain some degrees on the thermal objectives and reduce pressure drop and weight. This methodology can be extended to more complicated shape as shown on a curved cold-plate.

As these simulations on porous media run fast, it will be possible to apply an automatization that will help the engineer for enhancing performances or modify a he wishes the geometry. Finally, heat exchanger manufacturers will gain in times on the whole supply chain.

REFERENCES

- CHEN, M. (2015). *Design, Fabrication, Testing and Modeling of a high temperature Printed Circuit Heat Exchanger*. Thesis: The Ohio State University.
- HUGO, J.-M. (2012). *Transferts dans les milieux cellulaires à forte porosité : applications à l'optimisation structurale des échangeurs à ailettes*. Ph. D. Aix-Marseille Université.
- HUGO, J.-M. (2019). HEWAM – Heat Exchanger With Additive Manufacturing. *Paris Air Show 19*. LinkedIn. Retrieved from LinkedIn: <https://www.linkedin.com/pulse/hewam-heat-exchanger-additive-manufacturing-jean-michel-hugo/?trackingId=fuVyJlXaQqOpZB4w6IDf0A%3D%3D>

LANGNAU, L. (2016). *Metal additive manufacturing enables lean, green heat exchanger*. Retrieved from makepartsfast.com: <https://www.makepartsfast.com/metal-additive-manufacturing-enables-lean-green-heat-exchanger/>

Magistrelli, G. (2019). Aeronautics and additive manufacturing still inseparables in 2019. *A3DM n°21*, 18-22.

Velo3D. (2018, November 13). *Formnext annonce*. Retrieved from Twitter: https://twitter.com/Velo_3D/status/1062300351896915968

Whitaker, S. (1998). *The Method of Volume Averaging*. Springer.